HHS Public Access

Author manuscript

Gene Ther. Author manuscript; available in PMC 2016 May 18.

Published in final edited form as:

Gene Ther. 2016 February ; 23(2): 196–204. doi:10.1038/gt.2015.93.

Photoreceptor Rescue by an Abbreviated Human *RPGR* Gene in a Murine Model of X-linked Retinitis Pigmentosa

Basil S. Pawlyk[1,*], **Michael Adamian**[1], **Xun Sun**[4], **Oleg V. Bulgakov**[4], **Xinhua Shu**[3], **Alexander J. Smith**[5], **Eliot L. Berson**[1], **Robin R. Ali**[5], **Shahrokh Khani**[2], **Alan F.Wright**[3], **Michael A. Sandberg**[1], and **Tiansen Li**[4,*]

[1] Berman-Gund Laboratory for the Study of Retinal Degenerations, Harvard Medical School, Massachusetts Eye and Ear, Boston, MA, 02114

[2] Schepens Eye Research Institute, Harvard Medical School, Massachusetts Eye and Ear, Boston, MA, 02114

[3] MRC Human Genetics Unit, University of Edinburgh, UK

[4] National Eye Institute, Bethesda, Maryland, 208092

[5] Department of Genetics, University College London Institute of Ophthalmology, London, UK

Abstract

The X-linked *RP3* gene codes for the ciliary protein RPGR and accounts for over 10% of inherited retinal degenerations. The critical *RPGR-ORF15* splice variant contains a highly repetitive purine-rich linker region that renders it unstable and difficult to adapt for gene therapy. To test the hypothesis that the precise length of the linker region is not critical for function, we evaluated whether AAV-mediated replacement gene therapy with a human *ORF15* variant containing in-frame shortening of the linker region could reconstitute RPGR function *in vivo*. We delivered human *RPGR-ORF15* replacement genes with deletion of most (314-codons, “short form”) or 1/3 (126-codons, “long form”) of the linker region to *Rpgr null* mice. Human *RPGR-ORF15* expression was detected post-treatment with both forms of *ORF15* transgenes. However, only the long form correctly localized to the connecting cilia and led to significant functional and morphological rescue of rods and cones. Thus the highly repetitive region of RPGR is functionally important but that moderate shortening of its length, which confers the advantage of added stability, preserves its function. These findings provide a theoretical basis for optimizing replacement gene design in clinical trials for X-linked *RP3*.

*Correspondence to: Basil S. Pawlyk, Berman-Gund Laboratory, Massachusetts Eye and Ear, 243 Charles Street, Boston, MA 02114. Phone: (617) 573-3608; ; Email: Basil_Pawlyk@meei.harvard.edu or Tiansen Li, National Eye Institute, 6 Center Drive, Bethesda, MD20892. ; Email: tiansen.li@nih.gov. Phone: (301) 443 2833

Author Disclosure Statement

The authors declare that “No competing financial interest exists”.

Supplementary Information is available at Gene Therapy website (http://www.nature.com/gt)

Introduction

Retinitis pigmentosa (RP) is a leading form of inherited blindness in humans, with three general modes of inheritance (autosomal dominant, autosomal recessive, and X-linked). Over 70% of X-linked RP (and up to 20% of all RP cases) are caused by mutations in the gene encoding retinitis pigmentosa GTPase regulator (RPGR)[1-4], which involves both rod and cone photoreceptors as primary targets[5] and particularly impacts central vision[6]. Its high frequency and associated central visual handicap make *RPGR* an important RP disease gene.

RPGR is expressed in a complex pattern, with both default and ORF15 variants having been described[7]. The default or constitutive form of *RPGR* spans exons 1-19 and ORF15 terminates in a large alternative exon designated ORF15 excluding exons 16-19. The ORF15 exon is unique in that it contains a long purine rich repetitive sequence that proved impossible to clone into cDNA from retinal RNA and unstable in many procedures of recombinant DNA manipulations. The repetitive region is highly charged with a large number of glutamic acid residues and serves as a linker connecting the conserved N-terminal RCC1 homology domain and a C-terminal domain with no known functional motifs. While the smaller default form of RPGR is the predominant form in most tissues with primary or motile cilia[8], the ORF15 isoform of RPGR is necessary for normal rod and cone function in the retina[7, 9] and is expressed primarily in photoreceptors[8]. The ORF15 region is a mutation hotspot in *RPGR*, with mutations identified in this region in up to 60% of patients with X-linked RP[7, 10, 11].

We developed the first mouse model of X-linked RP carrying a null mutation in *Rpgr* with no detectable levels of any isoforms of RPGR[5]. *Rpgr null* mice manifest a slowly progressive retinal degeneration that is characterized by early cone opsin mislocalization in cell bodies and synapses and reduced levels of rhodopsin in rods. By 12 months of age significant photoreceptor cell loss and decline in cone and rod function, as measured by electroretinograms (ERG), become apparent. In the retina, RPGR is bound to the photoreceptor connecting cilium via an RPGR interacting protein (RPGRIP1)[12-14]. The connecting cilium is analogous to the transition zone of motile or primary cilia that serves as a gateway for protein trafficking to the outer segment. This subcellular localization pattern and the mutant mouse phenotype suggest that RPGR may have a role in protein trafficking between the inner and outer segment of both rods and cones[5, 14, 15]. In attempts to develop an *Rpgr* mutant mouse model with a faster course of degeneration, several other *Rpgr* mouse lines have been recently developed[16, 17]. There has also been a recent report of a naturally occurring model (rd9) of X-linked Rpgr[18]. In all of these cases, including the *Rpgr null*, mice display a slowly progressive loss of photoreceptors and varying degree of rod and cone involvement that may be due, in part, to differences in strain and/or pigmentation. These findings indicate that the slow rate of degeneration in the knockout model is due to species differences rather than the ablation being incomplete, and support the applicability of this murine model in therapeutic studies of null *RPGR* mutations in patients.

We have previously demonstrated functional and morphological rescue of both rod and cone photoreceptor cells in mice lacking RPGR using an abbreviated murine *Rpgr ORF15* isoform and a transgenic approach[19]. The rationale for the abbreviated construct was two

fold. First, the abbreviated construct could be amplified by RT-PCR from mouse retina mRNA, whereas the published "full-length" form of *Rpgr ORF15* was not and therefore, was never verified as being actually present in nature. Second, the purine-rich repetitive linker region in the ORF15 15 exon rendered the sequence unstable and hence prone to spontaneous deletions or rearrangements that could generate disease-causing frame shift mutations (unpublished observations). Since variation in the length of the repetitive region is frequently found in normal individuals[1, 20, 21], the precise length of the repetitive region appears not to be critical for function. Our previous mouse study using a murine *Rpgr ORF15* that is shortened by one third in the linker region supports this notion[19]. Therefore, an argument could be made that trading off some length (in-frame) of this region for added stability may be of net benefit because it generates a safer and still efficacious replacement gene construct. These considerations prompted us to explore this idea further. In the present study, we tested if a shortened human *RPGR ORF15* replacement gene, driven by our previously characterized rhodopsin kinase (RK) promoter[22, 23] and delivered in the AAV8 vector that expresses transgenes faster and displays favorable tropism toward photoreceptors[24, 25], would rescue photoreceptor degeneration in the *Rpgr* null mice. The results of the study shows that the purine-rich repetitive region of ORF15 exon is required for correct subcellular localization and full function of RPGR, but that moderate shortening of its length is well tolerated. These data lend credence to the proposal that a shortened *RPGR ORF15* replacement gene may offer a viable alternative to the thus far elusive "full-length" *RPGR ORF15* in future human gene therapy trials.

Results

AAV-mediated expression of human RPGR ORF15

We constructed two human *RPGR ORF15* replacement genes, one with an in-frame deletion of 126 codons (long form, *ORF15-L*) and the other with an in-frame deletion of 314 codons (short form, *ORF15-S*). Both were inserted into an AAV8 vector under the control of a human rhodopsin kinase promoter (Fig. 1A) [22, 23]. Subretinal delivery of the two human *RPGR ORF15* replacement genes led to the production of recombinant RPGR protein. By western blotting, 2 weeks following AAV vector administration, ORF15-L appeared as an ~ 160-kD protein while ORF15-S produced an ~ 130-kD protein. Both protein products were smaller than endogenous human ORF15 seen in human retinal extract (~ 200 kD) (Figs. 1B). Both forms of replacement ORF15 appeared as a single band when probed with an antibody against the C-terminus of human RPGR. Under our experimental conditions and the dosages given, the expression levels of ORF15-S and ORF15-L were comparable.

Both forms of ORF15 could be seen in the retina of $Rpgr^{-/-}$ mice by immunofluorescence staining of unfixed cryosections (3 weeks following subretinal injections). ORF15-L correctly localized to a narrow band in between the inner and outer segments where the connecting cilia reside. However, ORF15-S gave much weaker signals at the CC (Fig. 2A) than ORF15-L. In well-transduced retinal areas the signal from ORF15-L treated retinas appeared indistinguishable from the WT signal (Fig. 2A, B). Double-labeling with an antibody for the ciliary rootlets, which originate from the proximal ends of basal bodies and extend toward the cell interior and thus serve as a marker for the ciliary region [8, 26],

confirmed the correct subcellular localization of the recombinant RPGR to the connecting cilia (Fig. 2B). In contrast to the robust protein expression determined by western blotting, only ORF15-L appeared to have a robust signal in every CC matching the number of rootlets, whereas ORF15-S treated retinas, many rootlets did not have an RPGR signal at their distal ends. Figure 2C shows a bar graph representing RPGR label counts relative to the counts of rooteletin fibers in *Rpgr*$^{-/-}$ mouse retinas treated with either the long or short form of human ORF15 as well as in untreated wildtype mouse retinas. There was no difference in the mean ratios (RPGR signal count divided by Rootletin fiber count) for the ORF15 long form versus the wild type (Dunnett's method, $p = .24$) but a significantly lower mean ratio for the ORF15 short form versus the wildtype ($p = .0019$). Given the somewhat similar level of expression by immunoblotting, this disparity in protein localization at the connecting cilium suggested a somewhat reduced affinity of ORF15-S for the CC. Further analysis by immunostaining of fixed retinal sections, which afforded better preservation of tissues at the expense of signal strength at the CC, revealed a pattern of ORF15-S mislocalized to photoreceptor inner and outer segments (Fig. 2D). No mislocalization was seen for ORF15-L, which had a staining pattern similar to WT. Thus, the lack of staining for the short form RPGR at the CC was due to a reduced ability to localize to this subcellular compartment, rather than a lower level of expression overall.

Human ORF15-L expression in Rpgr null mice promotes rod and cone survival

To investigate a therapeutic efficacy of the two replacement genes, we evaluated *Rpgr*$^{-/-}$ mouse photoreceptors by immunostaining to look for signs of improvement in rod and cone morphology. By 13 months of age (6 months post treatment), both control and *ORF15-S* treated eyes had the typical degenerative appearance for this age (Fig. 3). Rod and cone outer segments were shortened and disorganized compared to WT eyes, with rod opsin mislocalization seen throughout the outer nuclear layer and cone opsin mislocalization in the synaptic layer. The outer nuclear layer was also comparably reduced in thickness in control and *ORF15-S* treated eyes. In contrast, eyes treated with *ORF15-L* had rhodopsin expression in rods that was properly partitioned to the outer segments with no obvious signs of mislocalization. Similarly, cone photoreceptor survival was enhanced following treatment with the longer *ORF15* construct, with rare cone opsin mislocalization. In addition, *ORF15-L* treated eyes were found to have more cells (with nearly normal-appearing rod and cone outer segments) than control or *ORF15-S* treated eyes. Based on these findings longitudinal studies were carried out in mice treated with *ORF15-L*.

We measured the thickness of the outer nuclear layer (ONL) and the length of photoreceptor inner/outer segments in both eyes of 3 *Rpgr*$^{-/-}$ mice. These were measured in 3 regions of the superior hemisphere and in 3 regions of the inferior hemisphere, each region separated by 600μm and beginning 600 μm to either side of the optic nerve head along the vertical meridian. Repeated-measures full-factorial regression at ages 11 months and 18 months was used to identify differences by eye, hemisphere, and region as main effects, as well as their cross-products to determine whether a treatment effect varied geographically. At 11 months of age, ONL thickness was normally distributed but inner segment/outer segment length was not (Shapiro-Wilk W goodness of fit test, $p = .016$); at 18 months of age, neither ONL thickness nor inner segment/outer segment length was normally distributed ($p = .0011$ and p

= .0002, respectively). At 11 months of age, mean ONL thickness was significantly greater for treated eyes (48.0 μm) than for control eyes (38.0 μm, p = .0015); mean inner segment/outer segment length was also significantly greater for treated eyes (45.1 μm) than for control eyes (29.5 μm, p < .0001, p < .0001 for normalized ranks). No other effect was statistically significant. At 18 months of age the differences in retinal morphology between fellow eyes were even more marked: mean ONL thickness was 22.8 μm for treated eyes and 13.7 μm for control eyes (p < .0001, p < .0001 for normalized ranks), while mean inner segment/outer segment length was 19.8 μm for treated eyes and 7.3 μm for control eyes (p < .0001, p < .0001 for normalized ranks). At this age we initially observed that the treatment benefit for IS/OS length was significantly greater in the superior retina than in the inferior retina at 18 months (p = .0036), but this did not hold up after converting length to normalized ranks (p = .17). Figure 4A illustrates ONL thickness and IS/OS length by region for treated and control eyes at 18 months of age.

Figure 4B shows representative light micrographs taken from a representative ORF15-L treated and fellow control eye at 18 months of age. In the control retina, the best-preserved area has only about 2-3 rows of loosely arranged photoreceptor nuclei with shortened and disorganized photoreceptor inner/outer segments. Note that the margins of the inner and outer segments are no longer distinct. The treated retina, on the other hand, has about 5-6 rows of photoreceptor cells throughout, with longer, better organized, and distinct inner and outer segments.

Human RPGR ORF15-L expression improves rod and cone function

Retinal function as monitored by full-field rod and cone ERGs was evaluated in a cohort (n=22) of *Rpgr*$^{-/-}$ mice from 9-months to 18-months of age. Mice received treatment between 3 and 7 months of age, and follow-up ERGs were recorded no sooner than 6-months following injection. Figure 5A shows rod and cone ERG amplitudes by eye for 16 mice tested between 11 and 14 months of age. Control eyes (OD) showed disproportionate loss of cone b-wave amplitude relative to rod b-wave amplitude compared with the lower limits for wild-type mice, as previously observed in this murine model of RPGR$^{-/-}$ mice (Hong and others, 2000) and evidence for a cone-rod degeneration. In every case but one, the treated eye (OS) had a larger a-wave and b-wave amplitude compared with the fellow control eye (OD), demonstrating improvement of rod and cone photoreceptor function. In fact, 56% of the treated eyes (9/16) had rod b-wave amplitudes that were at or above the lower limit of age-matched WT values (dotted line). Geometric mean values for rod ERG a-wave and b-wave amplitude were 121 μV OS and 65 μV OD for the a-wave and 482 μV OS and 267 μV OD for the b-wave. Mean cone ERG b-wave amplitudes were 22 μV OS and 11 μV OD. These data show an 81-86% improvement of rod function and a 100% improvement of cone function with AAV- *ORF15-L* treatment for this age range.

In the full cohort of 22 mice, we used repeated measures longitudinal regression to compare rates of change for log rod and cone b-wave amplitudes by eye (Fig. 5B). Estimated exponential mean rates of decline for rod b-wave amplitude were 8.6%/month in the control eyes and 3.8%/month in the treated eyes; the difference between these two means was significant (p=0.0001). Estimated exponential mean rates of decline for cone b-wave

amplitude were 5.8%/month in the control eyes and 0.8%/month in the treated eyes; the difference between these two means was also significant ($p<0.0001$), and the decline in cone b-wave amplitude in the treated eyes was not significantly different from zero ($p = 0.54$) — indicating no observable progression or loss in cone function over this period.

Representative rod and cone ERGs are shown in figure 5C to illustrate waveforms in treated and control eyes, including a WT, at 18 months of age (the final time point). In control eyes rod function was reduced, on average by 75%, while cone function was minimal and in some cases non-detectable. In contrast, treated eyes retained substantial, though subnormal, rod and cone function.

Discussion

In the present study *Rpgr* null mice treated with human *RPGR ORF15-L* showed significant rescue of cone and rod photoreceptor cells and function. Remarkably, treated mice had stable cone function between 9 and 18 months of age. This is a particularly desirable outcome for potential application to patients with X-linked RP due to mutations in *RPGR*, especially those affecting exon 15 of the protein that can cause cone-rod degeneration (see supplemental data) [27,28]. Thus the ORF15-L variant appears functional and may have future application in translation to the clinic. Since rescue in *Rpgr* null mice in the present study following treatment was nonetheless incomplete, it remains possible that a full-length version of *RPGR ORF15* may lead to even better rescue. However, we do not believe that is necessarily the case, since all gene therapy attempts thus far, even under the most optimized conditions, have led to incomplete rescue. It is more likely that issues relating to vector gene transduction, percentage coverage of the retina, gene expression levels and age or stage of disease of intervention provide more plausible explanations for incomplete rescue as well as avenues for improving the therapeutic benefits of *RPGR* gene augmentation. Still, it should be pointed out that the level of remaining retinal function in our mice treated with the abbreviated human *RPGR ORF15-L* would be consonant with their retaining normal, or nearly normal, visual fields to a large test light and, therefore, considerable mobility — based on the relationship between visual field size and ERG amplitude in RP patients [29].

Viral vector-mediated somatic gene therapy has shown great promise in treating animal models of human retinal degenerative disease. To date, there have been a number of successful studies using adeno-associated virus (AAV)-mediated gene delivery to rescue photoreceptor degeneration in rodent models [30–34] and in larger animal models [35–39]. In addition, Phase I clinical trials involving gene therapy for patients with Leber Congenital Amaurosis (LCA) targeting the RPE [40–42] and more recently choroideremia [43] have already met with some success. Mutations in *RPGR* are one of the most common causes of all forms of retinitis pigmentosa [4] and are associated with a more severe loss of central vision than most other genotypes. Hence *RPGR* is of great interest as a target for gene therapy development. There have been two reports of using full-length human *RPGR ORF15* for replacement gene therapies in the canine and mouse models of X-linked RP[37, 44]. There are currently no clinical trials using AAV-mediated gene replacement therapy for the treatment of patients with X-linked RP, but such trials are likely to be underway in the near future.

For a successful implementation of *RPGR* replacement gene therapy, a number of issues need to be considered. First, RPGR is required for both rod and cone survival. Therefore, the replacement gene expression needs to be driven by a cell type specific promoter that is active in rods and cones, but not in RPE cells. The RK promoter used in this study appears to fulfill this requirement. A similar RK promoter design has been previously shown to drive gene expression efficiently in both rod and cone photoreceptors [22]. In the present study, robust protein expression was seen for both abbreviated forms of RPGR ORF15 as evidenced by IHC and Western blotting data. By Western blotting both forms of ORF15 were expressed at levels that were similar to or slightly above that seen in a normal human retina. By immunofluorescence, both forms of ORF15 were found exclusively in the photoreceptor cells, and absent in the RPE or the inner retina. Thus the replacement gene constructs used in this study were able to drive expression in the target cells and at levels that are likely appropriate for therapeutic studies. The combination of the fast acting AAV8 delivery vector and our human RK promoter has been previously used to rescue photoreceptor degeneration in two murine models of Leber congenital amaurosis (AIPL1 and RPGRIP1) [23, 31, 33]. This strategy is likely to be useful in future clinical studies for *RPGR* gene replacement.

The second issue is the choice of the replacement gene sequence that is to be incorporated into the vector construct. More often than not, multiple transcript variants will be expressed from a single gene due to alternative splicing or transcriptional start and termination. Alternative splicing underlies the evolution of increased proteomic and functional complexity and is especially prevalent in neural tissues. For *RPGR*, this issue is particularly acute because of its complex expression patterns. It is now widely accepted that the *ORF15* variant is the functional important isoform in photoreceptors and should be the choice for any gene therapy attempt. However, the *ORF15* variant of *RPGR* contains a long stretch of highly repetitive, purine-rich region that makes it difficult to be reverse transcribed into cDNA and prone to deletions and rearrangements during plasmid propagation. These same traits probably render it a mutation hot spot in humans. Thus the stability of the ORF15 region is a concern for human *RPGR* gene therapy. It remains unclear why the *ORF15* region is so unstable or difficult to clone. Analysis of this region shows that the purine-rich sequence has a strong potential for forming multiple, stable G-quadruplexes. Such secondary structures will likely interfere with reverse transcription and DNA replication. The repetitive nature of the sequence may also lead to polymerase slippage thus compromising fidelity of DNA replication. In a previous study with murine *ORF15* [19] a moderate in-frame shortening of this region (by 650 bp of nearly one half of the repetitive region in mouse *RPGR ORF15*) was shown to increase the stability of the cDNA. RPGR protein product from this abbreviated construct localized correctly to the photoreceptor connecting cilia and rescued the disease phenotype. Thus this shortened form of RPGR retained its function. In the current study, we delivered a human ORF15 that was shortened by about one third in the purine rich repetitive region, and found it to correctly localize to the connecting cilia of photoreceptors and rescue the disease phenotype. These findings show that the *ORF15-L* form of *RPGR* described in this study retains RPGR function *in vivo*. In contrast, the *ORF15-S* form had lost most of the purine rich region, and was found unable to localize to the connecting cilia efficiently and failed to rescue the disease phenotype. Thus, while shortening of the purine rich region by about one third may promote photoreceptor rescue in

patients with RPGR mutations, further reduction in the length of this region would not be expected to lead to this benefit. The conclusion that abbreviated *RPGR* could remain functional is also supported by other circumstantial evidence. First, there is considerable variation in the length of this region, albeit only by dozens of base pairs, among normal human retinas. Second, different mammalian species vary considerably in the length of this region. For example, this region is longer by about 200 base pairs in mice compared to humans. In comparison, the length of the RCC1 homology domain in the N terminal half of the protein, and the C terminal unique region are very similar between the species. Our data therefore provide a useful guideline on the design of an abbreviated human *RPGR ORF15* replacement gene for future clinical studies that affords both the benefit of increased stability and functionality.

The idea of using abbreviated genes for gene therapy is by no means a novel one. This strategy is currently being used in clinical trials to deliver a miniaturized version in lieu of the full-length dystrophin gene (14 kb) by AAV vectors, which have a packaging limit of about 4.7 kb, to patients afflicted with X-linked Duchenne muscular dystrophy. In the case of *RPGR*, the motivation for studying shortened versions is different. The full-length *RPGR ORF15* gene should have no difficulty fitting into existing AAV vectors. The shortened version of *RPGR ORF15*, by being both functional and more stable, will reduce the chances of gene rearrangements and the ensuing production of aberrant, frame shifted protein products, which are presumed to be deleterious to the photoreceptors. This in principle should enhance the margin of safety of the therapy. Miniaturized versions of large genes almost invariably come at a substantial cost in terms of compromised functions. This downside does not appear to apply to the shortened versions (both mouse and human) of RPGR ORF15, based on the in vivo studies that we have conducted. Thus the long version of *RPGR ORF15* presented in this study, with of its repetitive region removed for added stability, could serve as a viable alternative to the “full-length” *RPGR ORF15* in replacement gene therapies.

Materials and Methods

Animals

The generation and analysis of $Rpgr^{-/-}$ mice have been described previously (Hong and others, 2000). The (C57BL/6) $Rpgr^{-/-}$ mice used in this study were bred from backcrossing and sibling mating and were maintained in our institutional animal facility. WT mice used in the study were C57BL from Charles River Laboratory (Wilmington, MA). Mice were maintained under 12hr light/12hr dark lighting cycle. All mice were euthanized by CO_2 inhalation for collection of ocular tissues. The studies were done in accordance with the ARVO Statement for the Use of Animals in Ophthalmic and Vision Research, and approved by the IACUC of the Massachusetts Eye and Ear Infirmary.

Plasmid construction and production of recombinant AAV8

Human *RPGR ORF 15* cDNA was amplified from human retinal cDNA by PCR using primers designed to encompass the entire *RPGR ORF15* isoform coding region. No full-length *ORF15* cDNAs were obtained despite repeated attempts using a variety of methods,

consistent with the experience of other investigators and that of our own [19]. Instead, we obtained an abbreviated *ORF15* cDNA containing a large 314 codon (942 bp) in-frame deletion in the ORF15 exon (2,517-bp remaining) with the bulk of the purine rich repetitive region removed (codons 696-1010del, “short form”) (Fig. 1A). A second *ORF15* cDNA was constructed through recombinant DNA manipulation that contained a 126-codon (378 bp) in-frame deletion within the highly repetitive region of exon 15 (with 3,081-bp remaining in the ORF15 exon) (codons 862-988del,“long form”). These *ORF15* cDNAs were sequenced to verify fidelity. To construct the AAV vectors, RPGR cDNAs were inserted into the multiple cloning site of the parental pAAV-RK-zsGreen vector. The resulting *pAAV-RK-ORF15-L* and *pAAV-RK-ORF15-S* vectors were packaged into AAV8. AAV2/8 pseudotyped vector was generated by tripartite transfection: (1) AAV vector plasmid encoding the gene of interest, (2) AAV helper plasmid pLT-RC03 encoding AAV Rep proteins from serotype 2 and Cap proteins from serotype 8, and (3) adenovirus helper miniplasmid pHGTI-Adeno1) into 293A cells. The transfection was performed using a protocol developed by Xiao and co-workers [45]. Two days after transfection, cells were lysed by repeated freeze and thaw cycles. After initial clearing of cell debris, the nucleic acid component of the virus producer cells was removed by Benzonase treatment. The recombinant AAV vector particles were purified by iodixanol density gradient. The purified vector particles were dialyzed extensively against PBS and tittered by dot blot hybridization. The purified vectors are referred to as *AAV-ORF15-L* and *AAV- ORF15-L* in the remainder of the text.

Subretinal injections

Mice were placed under general anaesthesia with an intraperitoneal injection of ketamine (90 mg/kg)/xylazine (9 mg/kg). A 0.5% proparacaine solution was applied to the cornea as a topical anesthetic. Pupils were dilated with topical application of cyclopentolate and phenylephrine hydrochloride. Under an ophthalmic surgical microscope, a small incision was made through the cornea adjacent to the limbus using an 18-gauge needle. A 33-gauge blunt needle fitted to a Hamilton syringe was inserted through the incision behind the lens and pushed through the retina. Injections were made subretinally within the nasal quadrant of the retina. Each eye received either 2×10^9 vector genome (*AAV- ORF15-L*) or 5×10^9 vector genome (*AAV- ORF15-S*) in a 1 μl volume. RPGR-ORF15 vectors were administered to the left eye (OS, oculus sinister) and control vector (*AAV8-RK- EGFP*) were administered to the right eye (OD, oculus dexter). These are referred throughout this text as “treated” or “control”, respectively. Visualization during injection was aided by the addition of fluorescein (100mg/ml AK-FLUOR, Alcon, Inc.) to the vector suspensions at 0.1% by volume. Fundus examination following the injection showed > 50% of the retina detached in most cases, confirming successful subretinal delivery. Cohorts of mice (n=50 total) were injected at 1 month of age for protein expression studies and at 3 to 7 months of age (since ERGs remained normal during this age period) for functional (ERG) and histological studies, prior to major photoreceptor loss.

Histology and immunofluorescence

For light microscopy, enucleated eyes were fixed for 10 minutes in 1% formaldehyde, 2.5% glutaraldehyde in 0.1 M cacodylate buffer (pH7.5). Following removal of the anterior segments and lenses, the eyecups were left in the same fixative at 4°C overnight. Eyecups

were washed with buffer, post-fixed in osmium tetroxide, dehydrated through a graded alcohol series and embedded in Epon. Semi-thin sections (1 μm) were cut for light microscopy observations. For EM, ultrathin sections were stained in uranyl acetate and lead citrate before viewing on a JEOL 100CX electron microscope.

For immunofluorescence staining of ciliary proteins two methods were used. In one method, which yielded the strongest fluorescence signal, eyes were enucleated, shock frozen, and sectioned at 10-μm thickness in a cryostat. Unfixed frozen sections were then collected on glass and stained. In a second method, floating retinal sections were collected and stained. For this process eyes were placed in fixative (2% formaldehyde/PBS) and their anterior segments and lenses were removed. Duration of fixation was typically 20 minutes. The fixed tissues were soaked in 30% sucrose/PBS for at least 2 hours, shock frozen and sectioned similar to unfixed tissues. Sections were then collected into PBS buffer and remained free floating for the duration of the immunostaining process. For immunostaining of all other proteins only floating sections were collected and stained. Stained sections were viewed and photographed on a laser scanning confocal microscope (model TCS SP2; Leica). Antibodies used were mouse RPGR (S1), a human RPGR C-terminal antibody, anti-rootletin, 1D4 (anti-rhodopsin), mixed blue/green cone anti-opsin, and Hoechst 33342, nuclear dye stain.

Immunoblotting analysis

Retinal tissues were homogenized in RIPA buffer, boiled in Laemmli buffer and loaded at 15 μg/lane on 5% SDS-PAGE gels. After gel separation, proteins were blotted to PVDF membrane by electrotransfer. The membranes were blocked with 5% non-fat milk and incubated with primary antibodies overnight at room temperature. After washing, membranes were incubated with peroxidase-conjugated secondary antibodies. SuperSignal® West Pico Chemiluminescent Substrate (Pierce) was used for detection. For normalization, protein samples were separated on standard SDS-PAGE and probed with a transducin α antibody (gift of Dr. Heidi Hamm, Vanderbilt University).

ERG recording

Mice were dark-adapted overnight and anesthetized with sodium pentobarbital injected intraperitoneally prior to testing. Both pupils of each animal were topically dilated with phenylephrine hydrochloride and cyclopentolate hydrochloride, and mice were then placed on a heated platform. Rod dominated responses were elicited in the dark with 10-μs flashes of white light (1.37 cd•s /m^2) presented at intervals of 1 minute in a Ganzfeld dome. Light-adapted, cone responses were elicited with the same flashes presented at intervals of 1 Hz in the presence of a 41 cd/m^2 rod-desensitizing white background. ERGs were monitored simultaneously from both eyes with a silver wire loop electrode in contact with each cornea topically anesthetized with proparacaine hydrochloride and wetted with Goniosol, with a subdermal electrode in the neck as the reference; an electrically-shielded chamber served as ground.

All responses were differentially amplified at a gain of 1,000 (−3db at 2 Hz and 300 Hz; AM502, Tektronix Instruments, Beaverton, OR), digitized at 16-bit resolution with an adjustable peak-to-peak input amplitude (PCI-6251, National Instruments, Austin, TX), and

displayed on a personal computer using custom software (Labview, version 8.2, National Instruments). Independently for each eye, cone responses were conditioned by a 60 Hz notch filter and an adjustable artifact-reject window, summed (n=4-20), and then fitted to a cubic spline function with variable stiffness to improve signal:noise without affecting their temporal characteristics; in this way we could resolve cone b-wave responses as small as 2 μV.

Statistical analyses

ERG amplitudes were converted to natural logarithms to better approximate normal distributions. JMP Pro, version 11 (SAS Institute, Cary, NC) was used to compare cross-sectional ERG amplitudes and implicit times based on interocular difference scores, which were normally distributed by the Shapiro-Wilks W Goodness of Fit test. JMP Pro with Dunnett's method was used to compare RPGR expression divided by rootletin expression between wt mice (as control), mice injected with the short construct, and mice injected with the long construct; these ratio data were normally distributed. Repeated – measures regression with PROC MIXED OF SAS, version 9.3 (SAS Institute) or JMP Pro were used to compare ONL thicknesses and inner segment/outer segment lengths for treated versus untreated eyes at two ages. When these histologic data departed from normality, they were converted to normalized ranks by the Van der Waerden transformation and the regression analyses repeated. Repeated-measures regression was also used to compare rates of change of ERG amplitude over follow-up by eye. Using log data allowed these longitudinal ERG amplitudes to be fitted to a linear model consistent with the published exponential loss of ERG amplitude over time in mice with hereditary retinal degenerations[46].

Supplementary Material

Refer to Web version on PubMed Central for supplementary material.

Acknowledgment

We thank Dr. Jeng-Shin Lee at the Research Vector Core at Harvard Medical School for AAV vector packaging, and Drs. Peter Colosi and Zhijian Wu at the National Eye Institute for helpful discussions. This work was supported by National Eye Institute grant EY10581, NEI core grant for Vision Research (5P30EY14104), the Foundation Fighting Blindness, the Foundation for Retina Research, the Massachusetts Lions Eye Research Fund and by grants from the European Union (AAVEYE), the UK Department of Health, National Institute of Health Research BMRC for Ophthalmology, and UK Fight for Sight.

References

1. Bader I, Brandau O, Achatz H, Apfelstedt-Sylla E, Hergersberg M, Lorenz B, et al. X-linked retinitis pigmentosa: RPGR mutations in most families with definite X linkage andclustering of mutations in a short sequence stretch of exon ORF15. Invest Ophthalmol Vis Sci. 2003; 44(4):1458–63. [PubMed: 12657579]
2. Pelletier V, Jambou M, Delphin N, Zinovieva E, Stum M, Gigarel N, et al. Comprehensive survey of mutations in RP2 and RPGR in patients affected with distinctretinal dystrophies: genotype-phenotype correlations and impact on genetic counseling. Hum Mutat. 2007; 28(1):81–91. [PubMed: 16969763]
3. Branham K, Othman M, Brumm M, Karoukis AJ, Atmaca-Sonmez P, Yashar BM, et al. Mutations in RPGR and RP2 Account for 15% of Males with Simplex RetinalDegenerative Disease. Invest Ophthalmol Vis Sci. 2012; 53(13):8232–7. [PubMed: 23150612]

4. Churchill JD, Bowne SJ, Sullivan LS, Lewis RA, Wheaton DK, Birch DG, et al. Mutations in the X-linked retinitis pigmentosa genes RPGR and RP2 found in 8.5% offamilies with a provisional diagnosis of autosomal dominant retinitis pigmentosa. Invest Ophthalmol Vis Sci. 2013; 54(2): 1411–6. [PubMed: 23372056]
5. Hong DH, Pawlyk BS, Shang J, Sandberg MA, Berson EL, Li T. A retinitis pigmentosaGTPase regulator (RPGR)-deficient mouse model for X-linked retinitis pigmentosa(RP3). Proc Natl Acad Sci USA. 2000; 97(7):3649–54. [PubMed: 10725384]
6. Sandberg MA, Rosner B, Weigel-DiFranco C, Dryja TP, Berson EL. Disease course ofpatients with X-linked retinitis pigmentosa due to RPGR gene mutations. Invest Ophthalmol Vis Sci. 2007; 48(3): 1298–304. [PubMed: 17325176]
7. Vervoort R, Lennon A, Bird AC, Tulloch B, Axton R, Miano MG, et al. Mutational hotspot within a new RPGR exon in X-linked retinitis pigmentosa. Nature Genetics. 2000; 25(4):462–466. [PubMed: 10932196]
8. Hong DH, Pawlyk B, Sokolov M, Strissel KJ, Yang J, Tulloch B, et al. RPGR isoforms inphotoreceptor connecting cilia and the transitional zone of motile cilia. Invest Ophthalmol Vis Sci. 2003; 44(6):2413–21. [PubMed: 12766038]
9. Vervoort R, Wright AF. Mutations of RPGR in X-linked retinitis pigmentosa (RP3). Hum Mutat. 2002; 19(5):486–500. [PubMed: 11968081]
10. Breuer DK, Yashar BM, Filippova E, Hiriyanna S, Lyons RH, Mears AJ, et al. Acomprehensive mutation analysis of RP2 and RPGR in a North American cohort offamilies with X-linked retinitis pigmentosa. Am J Hum Genet. 2002; 70(6):1545–54. [PubMed: 11992260]
11. Sharon D, Sandberg MA, Rabe VW, Stillberger M, Dryja TP, Berson EL. RP2 andRPGR mutations and clinical correlations in patients with X-linked retinitis pigmentosa. Am J Hum Genet. 2003; 73(5):1131–46. Epub 2003 Oct 16. [PubMed: 14564670]
12. Boylan JP, Wright AF. Identification of a novel protein interacting with RPGR. Hum Mol Genet. 2000; 9(14):2085–2093. [PubMed: 10958647]
13. Roepman R, Bernoud-Hubac N, Schick DE, Maugeri A, Berger W, Ropers H-H, et al. The retinitis pigmentosa GTPase regulator (RPGR) interacts with novel transport-likeproteins in the outer segments of rod photoreceptors. Hum Mol Genet. 2000; 9(14):2095–2105. [PubMed: 10958648]
14. Hong DH, Yue G, Adamian M, Li T. Retinitis pigmentosa GTPase regulator (RPGR)-interacting protein is stably associated with the photoreceptor ciliary axoneme andanchors RPGR to the connecting cilium. J Biol Chem. 2001; 276(15):12091–12099. [PubMed: 11104772]
15. Hong DH, Li T. Complex expression pattern of RPGR reveals a role for purine-richexonic splicing enhancers. Invest Ophthalmol Vis Sci. 2002; 43(11):3373–82. [PubMed: 12407146]
16. Brunner S, Skosyrski S, Kirschner-Schwabe R, Knobeloch KP, Neidhardt J, Feil S, et al. Cone versus rod disease in a mutant Rpgr mouse caused by different geneticbackgrounds. Invest Ophthalmol Vis Sci. 2010; 51(2):1106–15. [PubMed: 20007830]
17. Huang WC, Wright AF, Roman AJ, Cideciyan AV, Manson FD, Gewaily DY, et al. RPGR-associated retinal degeneration in human X-linked RP and a murine model. Invest Ophthalmol Vis Sci. 2012; 53(9):5594–608. [PubMed: 22807293]
18. Thompson DA, Khan NW, Othman MI, Chang B, Jia L, Grahek G, et al. Rd9 is anaturally occurring mouse model of a common form of retinitis pigmentosa caused bymutations in RPGR-ORF15. PLoS One. 2012; 7(5):e35865. [PubMed: 22563472]
19. Hong DH, Pawlyk BS, Adamian M, Sandberg MA, Li T. A single, abbreviated RPGR-ORF15 variant reconstitutes RPGR function in vivo. Invest Ophthalmol Vis Sci. 2005; 46(2):435–41. [PubMed: 15671266]
20. Jacobi FK, Karra D, Broghammer M, Blin N, Pusch CM. Mutational risk in highlyrepetitive exon ORF15 of the RPGR multidisease gene is not associated with haplotypebackground. International journal of molecular medicine. 2005; 16(6):1175–8. [PubMed: 16273303]
21. Karra D, Jacobi FK, Broghammer M, Blin N, Pusch CM. Population haplotypes of exonORF15 of the retinitis pigmentosa GTPase regulator gene in Germany : implications forscreening for inherited retinal disorders. Molecular diagnosis & therapy. 2006; 10(2):115–23. [PubMed: 16669610]

22. Khani SC, Pawlyk BS, Bulgakov OV, Kasperek E, Young JE, Adamian M, et al. AAV-Mediated Expression Targeting of Rod and Cone Photoreceptors with a HumanRhodopsin Kinase Promoter. Invest Ophthalmol Vis Sci. 2007; 48(9):3954–61. [PubMed: 17724172]

23. Sun X, Pawlyk B, Xu X, Liu X, Bulgakov OV, Adamian M. Gene therapy with apromoter targeting both rods and cones rescues retinal degeneration caused by AIPL1mutations. Gene Ther. 2010; 17:117–131. [PubMed: 19710705]

24. Allocca M, Mussolino C, Garcia-Hoyos M, Sanges D, Iodice C, Petrillo M, et al. Noveladeno-associated virus serotypes efficiently transduce murine photoreceptors. J Virol. 2007; 81(20): 11372–80. [PubMed: 17699581]

25. Natkunarajah M, Trittibach P, McIntosh J, Duran Y, Barker SE, Smith AJ, et al. Assessment of ocular transduction using single-stranded and self-complementaryrecombinant adeno-associated virus serotype 2/8. Gene Ther. 2008; 15(6):463–7. [PubMed: 18004402]

26. Yang J, Liu X, Yue G, Adamian M, Bulgakov O, Li T. Rootletin, a novel coiled-coilprotein, is a structural component of the ciliary rootlet. J Cell Biol. 2002; 159(3):431–440. [PubMed: 12427867]

27. Demirci FY, Rigatti BW, Wen G, Radak AL, Mah TS, Baic CL, et al. X-linked cone-roddystrophy (locus COD1): identification of mutations in RPGR exon ORF15. Am J Hum Genet. 2002; 70(4): 1049–53. [PubMed: 11857109]

28. Yang Z, Peachey NS, Moshfeghi DM, Thirumalaichary S, Chorich L, Shugart YY, et al. Mutations in the RPGR gene cause X-linked cone dystrophy. Hum Mol Genet. 2002; 11(5):605–11. [PubMed: 11875055]

29. Sandberg MA, Weigel-DiFranco C, Rosner B, Berson EL. The relationship betweenvisual field size and electroretinogram amplitude in retinitis pigmentosa. Invest Ophthalmol Vis Sci. 1996; 37(8):1693–8. [PubMed: 8675413]

30. Pang JJ, Lei L, Dai X, Shi W, Liu X, Dinculescu A, et al. AAV-mediated gene therapy inmouse models of recessive retinal degeneration. Current molecular medicine. 2012; 12(3):316–30. [PubMed: 22300136]

31. Pawlyk BS, Bulgakov OV, Liu X, Xu X, Adamian M, Sun X, et al. Replacement genetherapy with a human RPGRIP1 sequence slows photoreceptor degeneration in a murinemodel of Leber congenital amaurosis. Hum Gene Ther. 2010; 21(8):993–1004. [PubMed: 20384479]

32. Pawlyk BS, Smith AJ, Buch PK, Adamian M, Hong DH, Sandberg MA, et al. Genereplacement therapy rescues photoreceptor degeneration in a murine model of Lebercongenital amaurosis lacking RPGRIP. Invest Ophthalmol Vis Sci. 2005; 46(9):3039–45. [PubMed: 16123399]

33. Tan MH, Smith AJ, Pawlyk B, Xu X, Liu X, Bainbridge JB, et al. Gene therapy forretinitis pigmentosa and Leber congenital amaurosis caused by defects in AIPL1: effective rescue of mouse models of partial and complete Aipl1 deficiency using AAV2/2and AAV2/8 vectors. Hum Mol Genet. 2009

34. Ali RR, Sarra GM, Stephens C, Alwis MD, Bainbridge JW, Munro PM, et al. Restorationof photoreceptor ultrastructure and function in retinal degeneration slow mice by genetherapy. Nat Genet. 2000; 25(3):306–10. [PubMed: 10888879]

35. Acland GM, Aguirre GD, Ray J, Zhang Q, Aleman TS, Cideciyan AV, et al. Genetherapy restores vision in a canine model of childhood blindness. Nat Genet. 2001; 28(1):92–5. [PubMed: 11326284]

36. Alexander JJ, Umino Y, Everhart D, Chang B, Min SH, Li Q, et al. Restoration of conevision in a mouse model of achromatopsia. Nat Med. 2007; 13(6):685–7. [PubMed: 17515894]

37. Beltran WA, Cideciyan AV, Lewin AS, Iwabe S, Khanna H, Sumaroka A, et al. Genetherapy rescues photoreceptor blindness in dogs and paves the way for treating human X-linked retinitis pigmentosa. Proc Natl Acad Sci U S A. 2012; 109(6):2132–7. [PubMed: 22308428]

38. Komaromy AM, Alexander JJ, Rowlan JS, Garcia MM, Chiodo VA, Kaya A, et al. Genetherapy rescues cone function in congenital achromatopsia. Hum Mol Genet. 2010; 19(13):2581–93. [PubMed: 20378608]

39. Lheriteau E, Libeau L, Stieger K, Deschamps JY, Mendes-Madeira A, Provost N, et al. The RPGRIP1-deficient dog, a promising canine model for gene therapy. Mol Vis. 2009; 15:349–61. [PubMed: 19223988]

40. Bainbridge JW, Smith AJ, Barker SS, Robbie S, Henderson R, Balaggan K, et al. Effectof gene therapy on visual function in Leber's congenital amaurosis. N Engl J Med. 2008; 358(21):2231–9. [PubMed: 18441371]

41. Cideciyan AV, Aleman TS, Boye SL, Schwartz SB, Kaushal S, Roman AJ, et al. Humangene therapy for RPE65 isomerase deficiency activates the retinoid cycle of vision butwith slow rod kinetics. Proc Natl Acad Sci U S A. 2008; 105(39):15112–7. [PubMed: 18809924]

42. Maguire AM, Simonelli F, Pierce EA, Pugh EN Jr. Mingozzi F, Bennicelli J, et al. Safety and efficacy of gene transfer for Leber's congenital amaurosis. N Engl J Med. 2008; 358(21):2240–8. [PubMed: 18441370]

43. Maclaren RE, Groppe M, Barnard AR, Cottriall CL, Tolmachova T, Seymour L. Retinal gene therapy in patients with choroideremia: initial findings from a phase 1/2clinical trial. Lancet. 2014

44. Wu Z, Hiriyanna S, Qian H, Mookherjee S, Campos MM, Gao C. A long-termefficacy study of gene replacement therapy for RPGR-associated retinal degeneration. Hum Mol Genet. 2015; 24(14):3956–70. [PubMed: 25877300]

45. Xiao X, Li J, Samulski RJ. Production of high-titer recombinant adeno-associated virusvectors in the absence of helper adenovirus. J Virol. 1998; 72(3):2224–32. [PubMed: 9499080]

46. Clarke G, Collins RA, Leavitt BR, Andrews DF, Hayden MR, Lumsden CJ, et al. A one-hit model of cell death in inherited neuronal degenerations. Nature. 2000; 406(6792):195–9. [PubMed: 10910361]

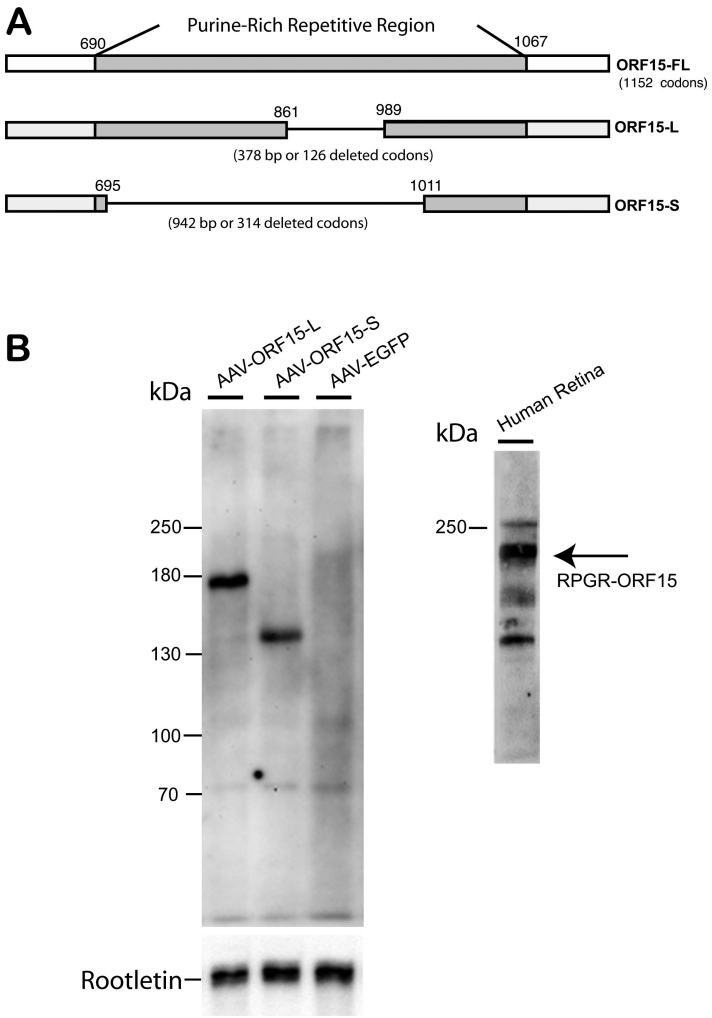

Figure 1.

(A) Maps of the native human *RPGR ORF15* coding region and both shortened forms of AAV-delivered human *ORF15*cDNA. **(B)** Immunoblots for the two recombinant forms of human *RPGR-ORF15*. AAV delivery of the small-deletion human cDNA (AAV-*ORF15-L*, "long form") leads to expression of a human RPGR-ORF15 protein of ~ 160 kD in size. AAV delivery of the large-deletion human cDNA (AAV-*ORF15-S*, "short form") leads to expression of a protein of ~130 kD in size. Both forms of human RPGR-ORF15 protein are smaller than endogenous human RPGR ORF15 found in human retinal tissue (~ 200 kD).

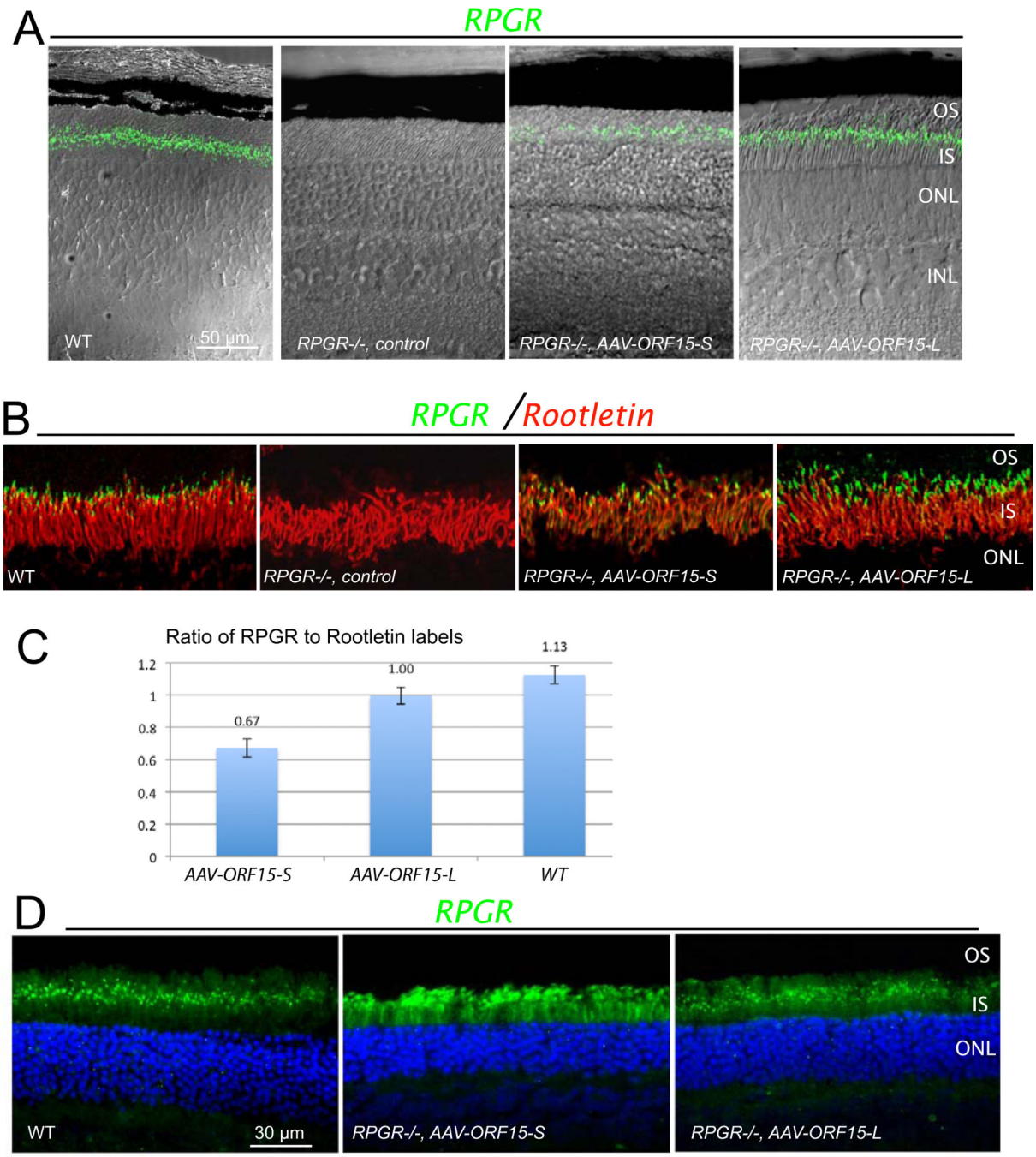

Figure 2.

RPGR ORF15 expression in *Rpgr*$^{-/-}$ mouse retinas following subretinal delivery of AAV-*RPGR ORF15*. (**A)** Fluorescence images of both the short (ORF15-S) and long (ORF15- L) forms of human RPGR ORF15 protein expression superimposed on Nomarski images to illustrate the layers of the outer retina. Staining of unfixed frozen retinal sections was performed at 3 weeks following treatment at 1-2 months of age. (**B)** Fluorescence images of both forms of human RPGR ORF15 co-localized with rootletin. Similar to WT, both forms of human RPGR ORF15 correctly localized to the photoreceptor connecting cilium just

distal to rootletin. RPE, retinal pigment epithelium; OS, outer segment; CC (TZ), connecting cilium (transition zone); IS, inner segment; ONL, outer nuclear layer. **(C)** Ratio of hRPGR fluorescent particles to fluorescent rootletin fibers at the connecting cilium for *Rpgr*$^{-/-}$ eyes (n=3) treated with ORF15-S, *Rpgr*$^{-/-}$ eyes (n=3) treated with ORF15-L, and wt eyes (n=3). Counts were obtained for both rootletin within the inner segment and RPGR just distal to rootletin over a 100μm length of midperipheral retina. Values are means ± 1 standard error). (**D)** Expression pattern of short and long form ORF15 protein in fixed floating retinal sections of *Rpgr*$^{-/-}$ mice. Sections were stained for human RPGR ORF15 protein localization 4-6 weeks following treatment at 2-3 months of age. In wt retina, murine RPGR ORF15 protein is seen as a discrete green fluorescent signal (dots) occupying the region between the photoreceptor inner and outer segments, at the level of the transition zone or connecting cilium. In contrast, the fluorescent signal for the short form of ORF15 (AAV-ORF15-S) is not limited to level of the photoreceptor connecting cilium but is also seen as diffuse signal throughout the inner and outer segments as well. The fluorescent signal for the long form of ORF15 shows very little, if any mislocalization, and is largely limited to the connecting cilium region similar to wt. OS, outer segment; CC (TZ), connecting cilium (transition zone); IS, inner segment; ONL, outer nuclear layer.

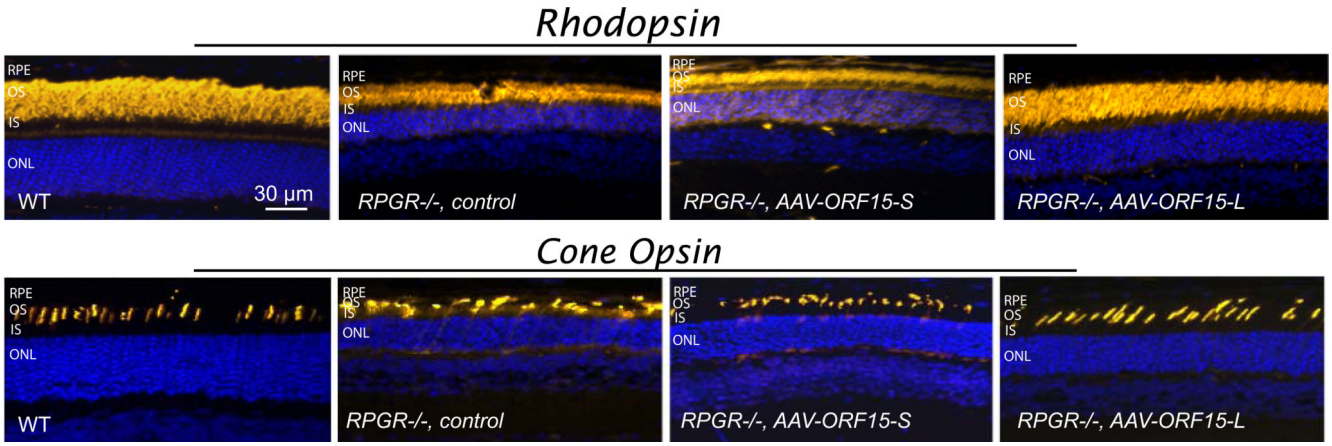

Figure 3.

Immunohistochemical (yellow) analyses of rod and cone photoreceptors in treated (short and long form of *ORF15*) and control $Rpgr^{-/-}$ mouse retinas at age 13 months (6-months post injection). In the $Rpgr^{-/-}$ mouse retina treated with the short form of ORF15 (AAV-*ORF15-S*), rhodopsin and cone opsin (mixed S & M cones in the inferior retina) mislocalization staining patterns are virtually indistinguishable from those seen in the control retina. Note the cone opsin mislocalization in the inner segments and synaptic layer in both of these mouse retinas.Similarly, rod and cone outer segments are shortened and disorganized with a reduced outer nuclear layer compared to an age matched wt retina. In contrast, in the $Rpgr^{-/-}$ mouse retina treated with the long form of ORF15 (AAV-*ORF15-L*) rhodopsin shows outer segment partitioning similar to WT mouse retina. Also in the *ORF15* long form treated retina rod outer segments are longer and well organized and the ONL is thicker compared with the control retina. Cone opsin staining shows more numerous cone photoreceptors with elongated and well-organized outer segments in the *ORF15* long form treated $Rpgr^{-/-}$ mouse retina compared with control.

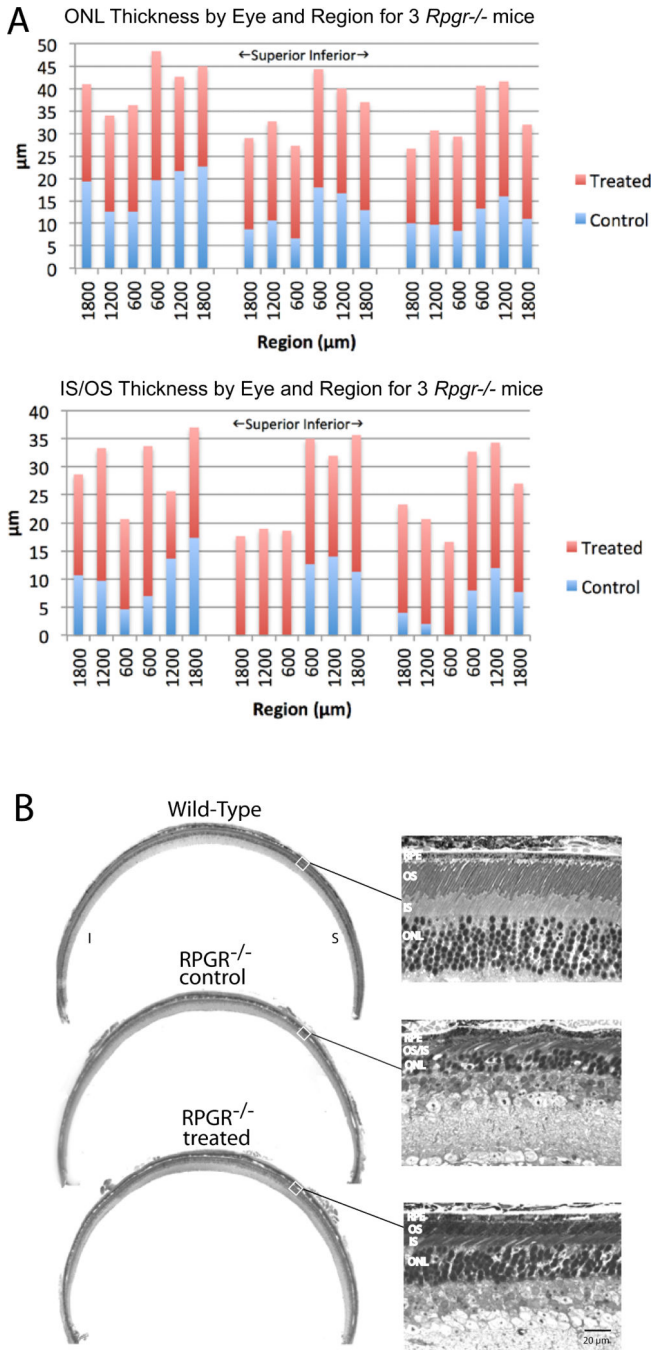

Figure 4.

Rescue of photoreceptor cells following treatment with *RPGR ORF15-L* in *Rpgr*$^{-/-}$ mice. (**A**) Shown are stacked bar graphs for ONL thickness (top) and IS/OS length (bottom) for treated (red) and fellow control (blue) eyes in 3 mice at 18 months of age. (**B**) Representative light micrographs from a WT mouse and an ORF15-L treated and fellow control eye from an *Rpgr*$^{-/-}$ mouse at 18 months of age. Images were taken from the mid periphery along the vertical meridian in the superior retina,

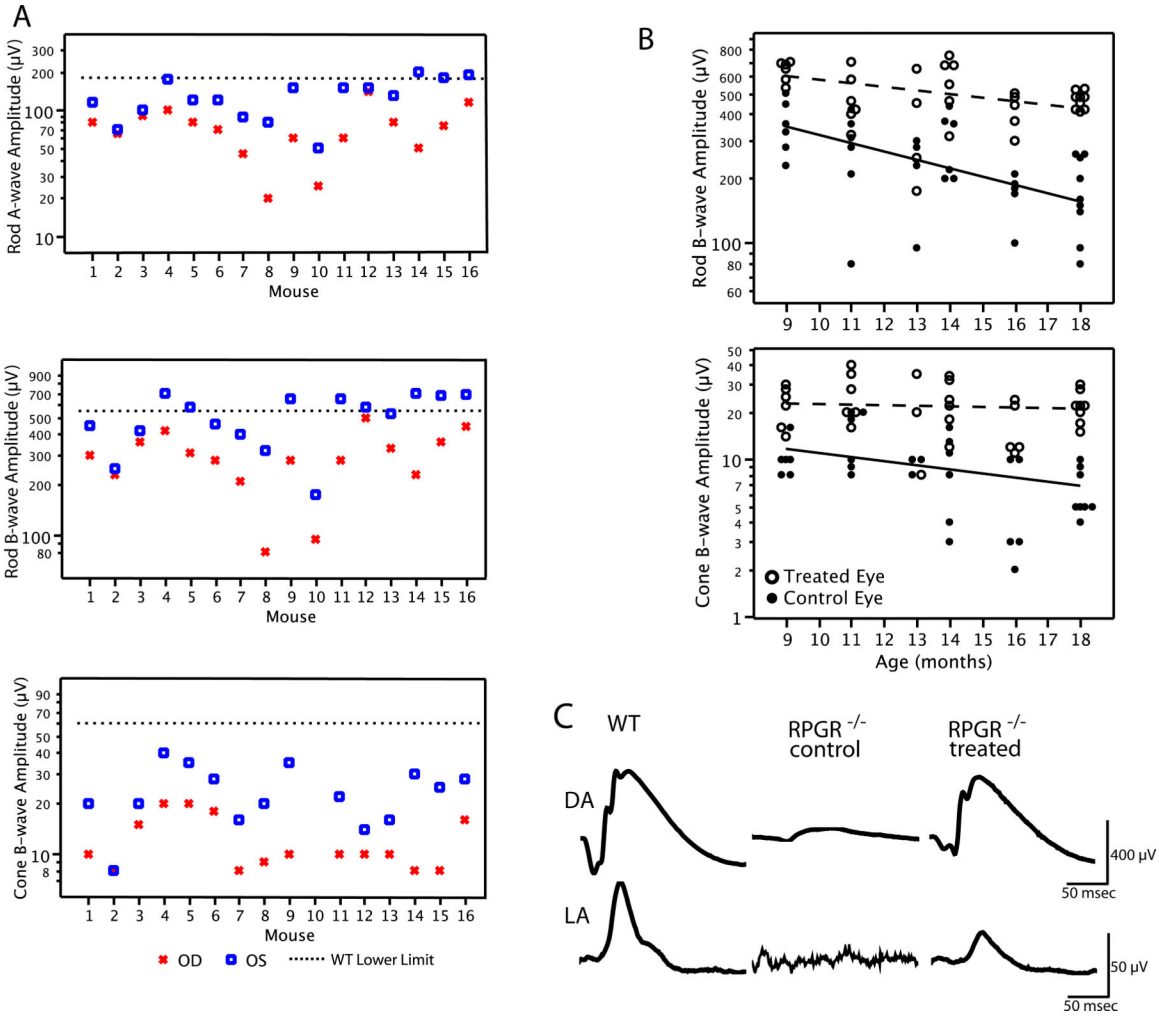

Figure 5.

(A) Rod a-wave, rod b-wave, and cone b-wave amplitudes from 16 *Rpgr*$^{-/-}$ mice at 11-14 months of age following treatment with *RPGR ORF15*-L. Control eyes (OD) showed disproportionate loss of cone b-wave amplitude relative to rod b-wave amplitude compared with the lower limits for wild-type mice. Mean values for all three measures were significantly different between eyes (p<0.001). **(B)** Scatterplots of ERG amplitude for 22 *Rpgr*$^{-/-}$ mice between 9 and 18 months of age on a log scale for the dark-adapted (rod) b-wave (upper graph) and light-adapted (cone) b-wave (lower graph) following treatment with RPGR ORF15-L. Data points have been shifted slightly horizontally for each age group to minimize data overlap. The regression lines for treated and control eyes were fitted by repeated measures longitudinal regression using PROC Mixed of SAS based on all available data. **(C)** Representative dark-adapted (DA) and light-adapted (LA) ERG waveforms from a pair of *ORF15-L* treated and fellow control *Rpgr*$^{-/-}$ eyes at 18 months of age. WT (age-matched) ERG waveforms are shown for comparison. ERG a-wave and b-wave are labeled *a* and *b*, respectively.